JOURNAL OF GEOPHYSICAL RESEARCH, VOL. 113, D00A05, doi:10.1029/2007JD009633, 2008

Estimating ice content and extinction in precipitating cloud systems from CloudSat radar measurements

Sergey Y. Matrosov[1,2] and Andrew J. Heymsfield[3]

Received 22 November 2007; revised 21 March 2008; accepted 2 June 2008; published 9 August 2008.

[1] Relations between W band radar reflectivity and ice cloud water content and visible extinction coefficient are developed using a large microphysical data set. These relations are specifically tuned for CloudSat radar to derive ice content and optical thickness of ice parts of precipitating systems where other types of measurements have limitations. Accounting for nonsphericity is essential for larger particles, which produce higher reflectivities ($Z_e > 0$ dBZ) and often dominate ice content of precipitating clouds. Typical values of median sizes in such clouds are about 1–2 mm, and they vary modestly. The modest particle size variability and strong non-Rayleigh scattering reduce data scatter in the derived relations and increase an exponent in best fit power law approximations for ice water content–reflectivity and extinction-reflectivity relations. The data scatter for high-reflectivity clouds is smaller than for low-reflectivity nonprecipitating clouds. It is about 33% for the reflectivity-ice water content relation, and it is about 50% for the reflectivity-extinction relation. For higher reflectivities, the temperature dependence of the ice water content-reflectivity relations is not very distinct, and uncertainties due to temperature variations are not expected to be high compared to possible errors due to particle shape variability. Uncertainties in particle aspect ratio, mass-size relation assumptions, and underrepresentation of smaller particles in samples can produce additional retrieval errors, so cloud ice content estimates can have uncertainties of about 50%, and extinction estimates can have uncertainties as large as a factor of 2.

Citation: Matrosov, S. Y., and A. J. Heymsfield (2008), Estimating ice content and extinction in precipitating cloud systems from CloudSat radar measurements, *J. Geophys. Res.*, *113*, D00A05, doi:10.1029/2007JD009633.

1. Introduction and Rationale

[2] Although CloudSat was originally designed for global observations of nonprecipitating clouds, it proved to be a valuable tool for quantitative precipitation estimations. Rain retrievals present certain challenges since signals at W band frequencies (~94 GHz) used for CloudSat's Cloud Profiling Radar (CPR) experience strong attenuation in rainfall. A number of approaches have been suggested for CloudSat-based rainfall retrievals. These approaches range from ones that use estimates of absolute values of CloudSat radar reflectivity factors (hereafter just reflectivities) [e.g., *L'Ecuyer and Stephens*, 2002] to those that are based on reflectivity gradients when attenuation is considered as a source of useful information rather than a factor hindering retrievals [e.g., *Matrosov*, 2007a]. While CPR-based rainfall retrievals are of particular interest, near surface snowfall estimates can also be obtained from CloudSat [*Matrosov et al.*, 2008].

[3] It might be expected in the near future that a combination of different CloudSat-based rainfall retrieval approaches can eventually provide reliable rain parameter estimates ranging from drizzle to some moderate rainfalls. Multiple scattering effects, however, will limit the maximum rain rates that are retrievable from CloudSat. Unlike for airborne W band radars [e.g., *Li et al.*, 2004], these effects are important for satellite measurements because of a coarser spatial resolution. They become progressively stronger as rain rate increases and ultimately dominate CloudSat signals from a rain layer with heavier rainfalls [*Battaglia et al.*, 2007].

[4] With a possibility of rainfall retrievals, CloudSat can provide quantitative information on the whole extent of a precipitating system including an ice cloud aloft. The complete vertical column retrieval information on such systems has not yet been available since precipitation radars (including a spaceborne radar that is used in the Tropical Rainfall Measuring Mission, TRMM) often do not have enough sensitivity for ice clouds, and zenith-pointing ground-based cloud radars have substantial problems observing the full extent of clouds through attenuating rain layers. CloudSat does not have these problems due its nadir-pointing observation geometry from space. It gives a unique opportunity to study precipitating systems as a whole thus

[1] Cooperative Institute for Research in Environmental Sciences, University of Colorado, Boulder, Colorado, USA.
[2] Earth System Research Laboratory, NOAA, Boulder, Colorado, USA.
[3] National Center for Atmospheric Research, Boulder, Colorado, USA.

0148-0227/08/2007JD009633$09.00

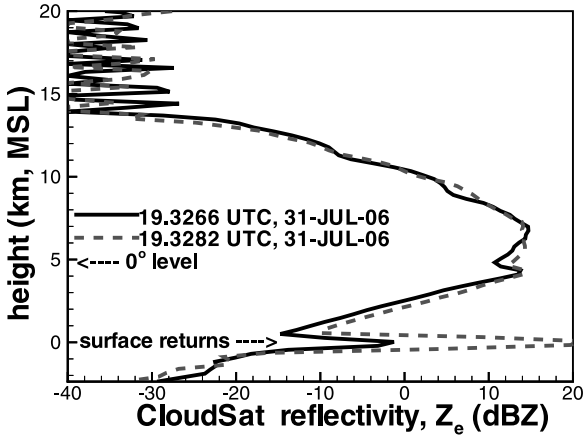

Figure 1. Vertical profiles of CloudSat reflectivity observed over a precipitating system on 31 July 2006.

providing observational insights in precipitation formation processes.

[5] An important parameter responsible for the ice cloud radiative and precipitation impacts is the ice water content (IWC), which is defined as the ice mass per unit volume of air. Two standard CloudSat algorithms provide IWC profiles (http://www.cloudsat.cira.colostate.edu). One of them uses CloudSat reflectivities and optical thickness estimates from the Moderate Resolution Imaging Spectroradiometer (MODIS), which is flown onboard of the Aqua satellite that is a part of the A-train. This algorithm could be generally inapplicable to precipitating systems because of serious limitations for optical thickness retrievals from passive sensors over rain. The other algorithm uses CloudSat measurements only and essentially relies on relations between the CloudSat reflectivity, Z_e, and IWC.

[6] The derivation of Z_e-IWC relations for cloud radars has more than 20 years of history [e.g., *Sassen*, 1987]. Some derivations have used model calculations based on in situ sampling data [e.g., *Liu and Illingworth*, 2000], while other approaches have also utilized data from multisensor retrievals and measured values of Z_e [e.g., *Matrosov*, 1997]. Two recent studies by *Hogan et al.* [2006] and *Protat et al.* [2007] developed CloudSat Z_e-IWC relations that depend on cloud temperature. Most of these derivations considered a wide range of Z_e and IWC, spanning several orders of magnitude and were chiefly oriented toward nonprecipitating clouds. W band radar measurements of ice parts of precipitating cloud systems, however, have their own specifics that are worth taking into account, and a special consideration of Z_e-IWC relations for such measurement situations is justified.

2. Specifics of W Band Radar Observations of Ice Parts of Precipitating Systems

[7] Figure 1 shows two vertical profiles of CPR measurements when CloudSat passed over a precipitating system near New Orleans, LA. The 0° isotherm for this case was located at about 4.8–4.9 km MSL and the typical rainfall rates in the layer below melting were about 4–5 mm h^{-1} [*Matrosov*, 2007a]. There was a clear bright band feature, which is often seen by CloudSat in the upper part of the melting layer of stratiform precipitations [*Sassen et al.*, 2007], and a small dark band just above this feature, which may have been caused by non-Rayleigh scattering effects on large ice crystals [*Heymsfield et al.*, 2008]. This precipitation system vertically extended to at least a 14 km height, above which the CloudSat reflectivity became noisy. The rapid decrease in observed reflectivity below about 4.2 km MSL is due attenuation in rain.

[8] Reflectivities measured by CloudSat in the ice part of the observed system reached a maximum value of about 14 dBZ, and they remained above 0 dBZ over an extended height interval. The fraction of total ice water path (IWP, defined as the vertical integral of IWC) from cloud parts with $Z_e > 0$ dBZ dominated the total IWP. This fraction is 96% and 97% for the profiles from Figure 1 if a generic ice cloud relation IWC (g m^{-3}) = 0.137 $Z_e^{0.64}$ (mm^6 m^{-3}) from [*Liu and Illingworth*, 2000] is used. On the basis of our experience, the example shown in Figure 1 is typical for CloudSat observations of precipitating systems. It indicates that ice cloud parts with $Z_e > 0$ dBZ observed over rainfall overwhelmingly contribute to the total ice content of precipitating systems (at least for those with rainfall rate values greater than several mm h^{-1}). This assumption, however, needs to be verified using global data in future studies.

[9] Most existing Z_e-IWC relations, including those dependent on temperature, were derived to cover a large dynamic range of possible values of both Z_e and IWC that occur in ice clouds ranging from thin cirrus to precipitating clouds. These values typically span 4–5 orders of magnitude, and a given relation would provide different uncertainties for different characteristic values of IWC. Typically data sets used for derivations have many more data points with $Z_e < 0$ dBZ than for larger reflectivity values. Given this, the corresponding relations could be more appropriate for nonprecipitating clouds. Deriving relations just for particular ranges of observed reflectivity (e.g., for those that determine IWP of ice parts of precipitating systems) would have a practical significance. This is especially true because practically all experimental data sets exhibit less data scatter at the high end of reflectivities and thus IWCs.

[10] Another important factor that influences the derivation of Z_e-IWC relations at W band frequencies is the nonsphericity of ice particles. Most developments that have utilized experimental cloud samples calculated reflectivity values using the Mie theory for spheres. It has been shown, however, that while particle nonsphericity impacts reflectivity in a relatively minor manner for the Rayleigh-type scattering, the effects of nonsphericity are much stronger for larger particles at W band where non-Rayleigh scattering effects are strong [*Matrosov*, 2007b]. Thus, accounting for nonsphericity effects should be an essential part of deriving CloudSat Z_e-IWC relations for ice parts of precipitating systems where particle sizes are usually large.

[11] The importance of accounting for ice particle nonsphericity at W band frequencies has also an experimental confirmation. It has been shown [*Matrosov et al.*, 2005] that dual-frequency radar ratio measurements (9.6 and 94 GHz) could not be explained by a spherical model, but a model for spheroids with an aspect ratio $r = 0.6$ was able to explain the observed data. Such aspect ratios were found to be

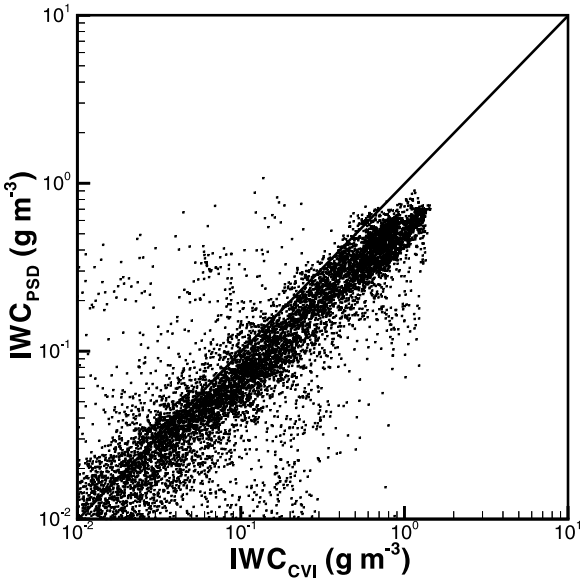

Figure 2. Comparisons of IWC values measured by the CVI probe and calculated from particle size distributions with $a = 0.0029$ and $b = 1.9$.

typical for ice particles that are greater than about 60 μm [*Korolev and Isaac*, 2003]. The spheroidal model is the simplest one that allows accounting for nonsphericity and has been extensively used to model backscatter properties of hydrometeors at radar frequencies [e.g., *Bringi and Chandrasekar*, 2001].

3. Experimental Data and Modeling Approach

[12] A large microphysical data set collected during the 2002 Cirrus Regional Study of Tropical Anvils and Cirrus Layers (CRYSTAL) Florida Area Cirrus experiment (FACE) was used in this study. Data were collected onboard the University of North Dakota Citation aircraft and they included samples from both precipitating and nonprecipitating clouds. Measurements by two-dimensional cloud and precipitation probes (2DC and 2DP) and a high-volume precipitation sensor (HVPS) provided ice particle size distributions (PSDs) in n = 33 bins covering a wide range of sizes from about 50 microns to several centimeters [*Heymsfield et al.*, 2005]. Aggregates were the most common particle habits, especially for larger sizes (more than few tenths of 1 mm), which contributed the most in ice cloud content for samples that resulted in higher reflectivity values.

[13] IWC values from PSD measurements were calculated from

$$\mathrm{IWC}\left(\mathrm{g\,m^{-3}}\right) = 10^6 \sum_{i=1}^{n} N_i(D_i) m_i(D_i), \tag{1}$$

where m_i and N_i are the mass of an individual particle (in grams) and particle concentration in ith size bin (per 1 cm^3), and D_i is the particle size (in centimeters) in terms of the maximum dimension. The summation is taken over all size bins. The mass m of an ice particle is represented by a power law relation

$$m(\mathrm{g}) = a\,D(\mathrm{cm})^b, \tag{2}$$

where values of the coefficients a and b describe a general particle population.

[14] The equivalent radar reflectivity was calculated from

$$Z_e\left(\mathrm{mm^6\,m^{-3}}\right) = 10^{12}\,\lambda^4\,\pi^{-5}\left|(\varepsilon+2)/(\varepsilon-1)\right|^2 \sum_{i=1}^{n} N_i(D_i)\sigma_i(D_i), \tag{3}$$

where λ (in cm), ε, and σ (in cm^2) are the radar wavelength, the dielectric constant of water at this wavelength, and the radar backscatter cross section, respectively. The coefficient 10^{12} in (3) converts cm^3 to mm^6 m^{-3}. The backscatter cross sections were calculated using the T-matrix approach [*Barber and Yeh*, 1975] which became a common tool for calculating scattering properties of nonspherical particles.

[15] Direct measurements of IWC (for IWC > 0.01 g m^{-3}) on the Citation aircraft were also available from a counterflow virtual impactor (CVI) probe. Figure 2 shows comparisons of IWC values measured by this probe and those calculated from PSDs using (1) and (2) with coefficients $a = 0.0029$ and $b = 1.9$ as suggested by *Brown and Francis* [1995] when mean particle dimension is used. These values of the coefficients have been widely used in different related studies. Results of Figure 2 show that PSD- and CVI-based IWC estimates agree reasonably well, although the values of the coefficients mentioned above result in a relatively small bias of IWC results from (1). This bias is about 0.83 for IWC > 0.1 g m^{-3}, and it is slightly less than that for lower ice water contents. On the basis of this comparison, the coefficient a was increased to $a = 0.0035$ for further estimates presented in this study (the value for b was left unchanged), so the bias between PSD- and CVI-based IWC estimates became negligible. Such fine-tuning of the coefficient a ensures that an *m-D* relation, which is proper for this data set, is used.

[16] An impact of the particle nonsphericity on radar reflectivity at W band is especially important for particles that are outside of the Rayleigh scattering regime. Such particles are typically observed in precipitating clouds. It was shown [e.g., *Matrosov*, 2007b] that populations of larger nonspherical particles with aspect ratios of $r = 0.6$ can result in reflectivities which are higher by 5–6 dB than those resulting from populations of spherical particles of the same mass. The nonsphericity is less important for particles that are within the Rayleigh scattering regime.

4. Z_e-IWC Relations for High Reflectivity Values

[17] Figure 3 shows scatterplots of W band reflectivity and IWC values derived from the PSD as discussed in section 3. The CloudSat sensitivity cutoff (−30 dBZ) was used as a threshold and the data are shown for spherical (Figure 3a) and spheroidal (Figure 3b) assumptions. An important feature of these plots is that the data scatter decreases as Z_e increases. It manifests in a narrowing area

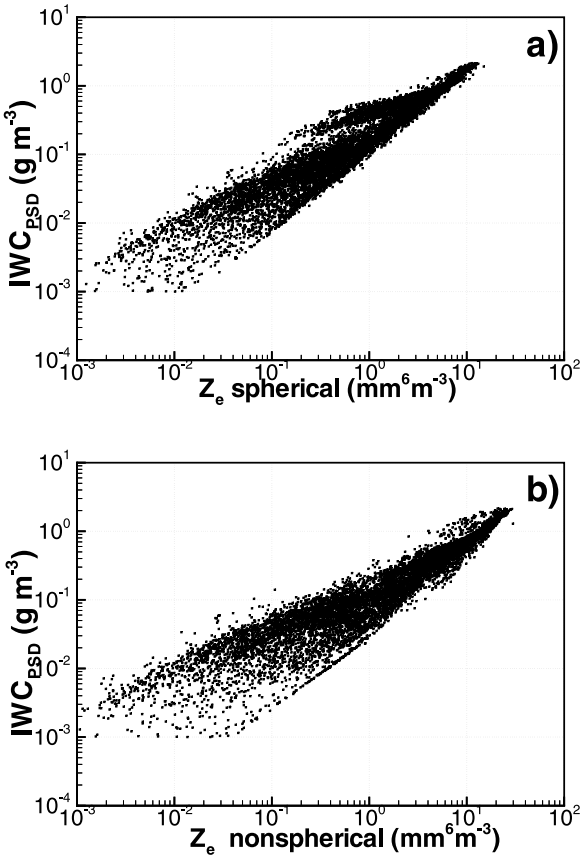

Figure 3. Scatterplots of IWC and W band reflectivity values derived for (a) spherical and (b) nonspherical (r = 0.6) particle assumptions.

of joint variability of IWC and Z_e as both parameters increase. Such narrowing is present in practically all published microphysical data sets [e.g., *Matrosov*, 1997; *Hogan et al.*, 2006; *Protat et al.*, 2007]. The data scatter gets progressively less as reflectivity increases.

[18] An important fact also is that the area of this narrowing in IWC and Z_e data is approximately the same in different data sets. Indeed, for a spherical assumption in Figure 3a, this area approximately stretches along a line connecting characteristic IWC and Z_e values of about 0.2 g m^{-3} and 1 mm^6 m^{-3} ($\sim$0 dBZ) and about 0.8 g m^{-3} and 4 mm^6 m^{-3} ($\sim$6 dBZ). The location of this area of the small data scatter is approximately the same for other data sets (but for the same shape assumption) from *Protat et al.* [2007, Figure 1] and *Hogan et al.* [2006, Figure 7]. Note that these authors also used microphysical data sets collected in midlatitude synoptically generated cloud systems. This correspondence between different microphysical data sets indicates that such narrowing and its location in the IWC-Z_e coordinates are consistent features that can be seen in cloud systems of various origin.

[19] The data scatter for lower values of IWC and Z_e is much more significant. Typical data sets also have many more data points for $Z_e < 0$ dBZ than for $Z_e > 0$ dBZ. This might mean that the Z_e-IWC relations (including those that account for temperature) derived using data, which vary in a large range of ice water content and reflectivity values, will provide better retrievals for lower reflectivities, and uncertainties associated with larger reflectivity measurements could be higher. In a way, this point is illustrated by results of *Protat et al.* [2007] when they show a rapid increase of retrieval uncertainties for IWC > 0.1 g m^{-3} [*Protat et al.*, 2007, Figure 3].

[20] Since for precipitating cloud systems, the reflectivity values $Z_e > 0$ dBZ are of the main interest, Figure 4 shows the scatterplot for the data using a 0 dBZ threshold. The best fit power law approximation for all the data in Figure 4 (r = 0.6) is

$$\mathrm{IWC}\left(\mathrm{g\,m^{-3}}\right) = c\,Z_e^d\left(\mathrm{mm^6\,m^{-3}}\right), \tag{4}$$

where c = 0.086 and d = 0.92 (note that c = 0.06 and d = 0.8 at K_a band). The relative standard deviation of IWC data around the best fit approximation is about 33%, and the relative bias is less than 5%.

[21] The temperature dependence of the Z_e-IWC relation for the 0 dBZ threshold is not very pronounced. Figure 5 shows the best fit power law approximations which are drawn for three different temperature intervals each containing more than a thousand data points. It can be seen that these approximations are rather close to each other, and they do not exhibit a consistent tendency for an increase or decrease in IWC estimates (for the same value of Z_e) as temperature changes from 0°C to −45°C. This fact indicates that the temperature information might be not very important when estimating ice cloud content from high reflectivities. This finding is in general accord with results of *Hogan et al.* [2006], who derived W band relations that produced quite different IWC values (depending on cloud temperature) for lower reflectivities but converged for higher values of Z_e [*Hogan et al.*, 2006, Figure 7c].

[22] For high reflectivity values, an uncertainty in particle nonsphericity can present a more important source of IWC retrieval errors than temperature variations. The results in Figure 4 are given for the aspect ratio r = 0.6. While this assumption appears to be appropriate given different experimental indications [e.g., *Korolev and Isaac*, 2003; *Matrosov et al.*, 2005], a possible uncertainty in (4) due to variability in r was estimated. The use of r = 0.8 rather than r = 0.6 (corresponding data are not shown) resulted in a reduction of

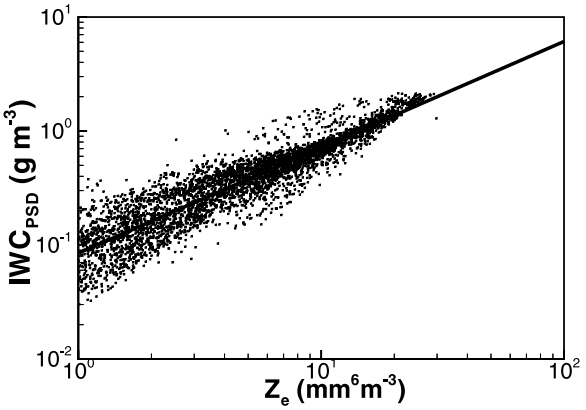

Figure 4. A scatterplot of IWC and W band reflectivity for nonspherical particles (r = 0.6) and a 0 dBZ cutoff.

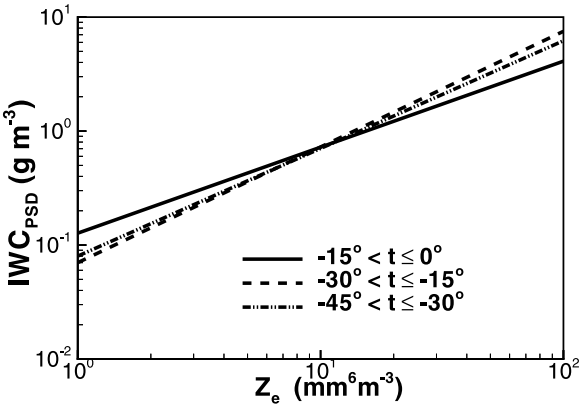

Figure 5. Best power law approximation fits for temperature stratified IWC-Z_e data shown in Figure 4.

reflectivity values for the same values of IWC, which caused an increase of the coefficient in (4) by about 25% while leaving the exponent practically unchanged.

[23] Another source of IWC retrieval errors is an uncertainty in the particle mass–size relation. Although the relation used here is appropriate for the considered microphysical data, there could be experimental situations when it will on average overestimate or underestimate particle mass and thus density. To estimate corresponding errors, a mean ice aggregate mass size relation $m = 0.003\ D^{2.15}$ from [*Mitchell*, 1996] was also used. The use of this relation resulted in about 30% variations in IWC retrievals compared to the mean estimator (4).

[24] The retrieval uncertainty can also increase if appreciable amounts of supercooled cloud water are present above the freezing level. While the unattenuated reflectivity contributions of cloud liquid is expected to be small because of the fact that cloud drops are generally much smaller than ice crystals, there will be some attenuation of CloudSat signals, which might result in underestimating of ice content. However, it is not common for stratiform precipitation (unlike for convective rains) to have significant amount of supercooled liquid.

4.1. Influence of Particle Characteristic Size on Data Scatter in Z_e-IWC Relations

[25] It can be shown that reflectivity can be approximated in terms of IWC and some characteristic size describing the whole PSD (e.g., the median volume particle size, D_0) as

$$Z_e = G\ \mathrm{IWC}\ D_0^{\beta}, \tag{5}$$

where G is a dimensionless parameter which is determined by the shape of the PSD and particle shape and density dependences. The exponent β is 3 for Rayleigh-type scattering [*Atlas et al.*, 1995] by constant density particles. As seen from (5), the data scatter in the Z_e-IWC relations should depend on the variability of D_0 and G. For particle populations with larger sizes, such as those observed in precipitating systems, the size distributions (and, as a result, reflectivity and IWC values) are often dominated by the large particle mode described by the exponential functions, and PSD changes for smaller particle sizes (<50–100 μm) are relatively unimportant. Given this, it can be expected that for a specific density assumption [$\rho \sim D^{-1.1}$ as determined by the mass-size relation (2), where mass increases as $D^{1.9}$ while the spheroidal volume increases as D^3], the data scatter in the Z_e-IWC relations will be dominated by the variability in the particle characteristic size.

[26] The data scatter is significant for smaller particles ($\beta \sim 3$), however, as characteristic size increases, the resonance scattering effects at W band become progressively stronger. This results in a much slower change of the backscatter cross section σ with D compared to the Rayleigh regime [*Matrosov*, 2007b; *Heymsfield et al.*, 2008], and in a corresponding reduction of β in (5). As a consequence, the variability in D_0 becomes less important for variability of reflectivity (5), and IWC and Z_e become more directly related. The lower data scatter and an increase in the value of the exponent d in the power law fit Z_e-IWC relations (compared to smaller particle populations) are manifestations of this mechanism. As mentioned above, this exponent is 0.92 in (4) for the high reflectivity values ($Z_e > 0$ dBZ) considered here, but it decreases to about 0.7 if the larger dynamic range of reflectivities is considered ($Z_e > -30$ dBZ).

[27] For reflectivity values of $Z_e > 0$ dBZ, which are of main interest in this study, Figure 6 shows a scatterplot between D_0 and Z_e. The presented data suggest that high values of IWC and Z_e, which are typical for ice parts of precipitating systems, usually come from particle populations consisting of larger crystals. For these higher Z_e values, there is no increasing trend of D_0 with Z_e as is often observed for lower reflectivities [e.g., *Matrosov*, 1997]. Typical values of D_0 in Figure 6 are about 1–2 mm. For such characteristic particle sizes, scattering at W band frequencies is essentially non-Rayleigh, and there are only modest changes of backscatter cross sections σ with particle size. Since particle bulk density diminishes with size as $D^{-1.1}$, a general trend of the backscatter cross section increase with size is smaller than D^2, which could be suggested for constant density particles. *Heymsfield et al.* [2006a] also observed similar particle size characteristics in high-reflectivity ice cloud parts of both synoptically generated and convective systems. This indicates that a lower variability of D_0 for high values of reflectivity is a common situation observed in clouds of different origin.

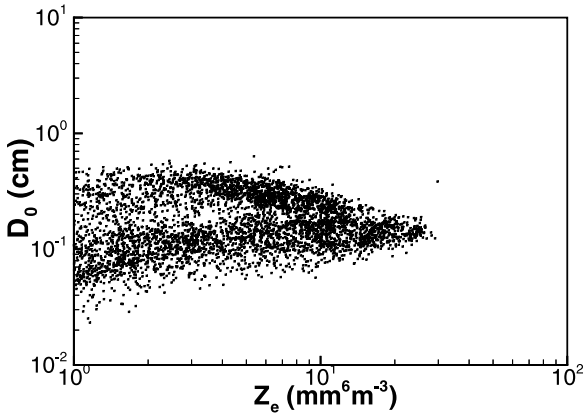

Figure 6. A scatterplot of median volume particle size D_0 and W band reflectivity ($r = 0.6$).

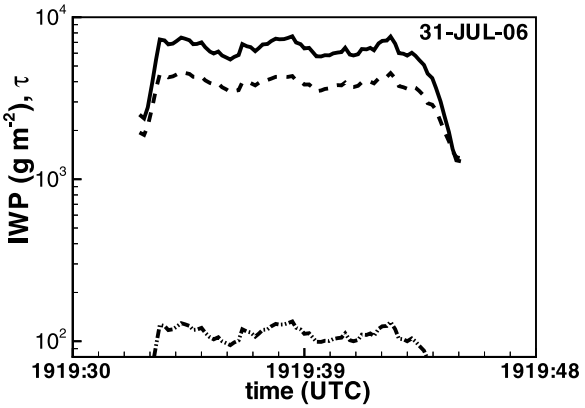

Figure 7. Retrievals of IWP and τ observed by CloudSat above the freezing level during the stratiform precipitation event on 31 July 2006. Solid line indicates results from the relation optimized for $Z_e > 0$ dBZ (IWC = 0.086 $Z_e^{0.92}$), dashed line indicates results from the best fit relation for $Z_e > -30$ dBZ (IWC = 0.115 $Z_e^{0.65}$), and dot-dashed line indicates optical thickness using (7).

[28] One interesting feature of Figure 6 is a slight decreasing trend of D_0 with Z_e for Z_e values that are greater than about 5 mm^6 m^{-3} ($\sim$7 dBZ). This can be explained by diminishing backscatter cross sections of larger particles due to resonance effects [e.g., *Matrosov*, 2007b]. This effect contributes to an existing data scatter in Z_e-IWC relations. Note that a related effect was also presented by *Heymsfield et al.* [2008], who reported a small decrease in observed W band reflectivities associated with non-Rayleigh scattering. They attributed it to the aggregational growth of ice particles beyond a size where the influence of the first backscatter resonance minimum becomes appreciable.

4.2. An Illustration of Retrievals

[29] An example of the retrieval of IWP values from CloudSat during a stratiform precipitating event observed on 31 July 2006 is shown in Figure 7. The retrievals correspond to the vertical atmospheric column above the freezing level which was observed by the CloudSat radar at altitudes about 4.8 km MSL and the estimated rainfall rates below the melting level were generally between 4 and 5 mm h^{-1} for the time interval 1919:34–1919:43 UTC. The rain layer retrievals for this event are described by *Matrosov* [2007a] where the corresponding time-height cross sections of CloudSat observations and rainfall rates are given. Two representative profiles of measured CloudSat reflectivity for this event are also shown in Figure 1.

[30] In addition to IWP retrievals obtained using the suggested in this study relation Z_e-IWC for $Z_e > 0$ dBZ, shown are also the results for the relation IWC = 0.115 $Z_e^{0.65}$ which was derived if the extended interval of all possible CloudSat reflectivities (>−30 dBZ) is considered as in Figure 3. Note that this extended interval relation is very close to the one suggested for 94 GHz by *Liu and Illingworth* [2000] (i.e., IWC = 0.137 $Z_e^{0.64}$) and fairly close to ones from *Hogan et al.* [2006] (e.g., IWC = 0.14 $Z_e^{0.8}$ for a −20°C temperature). Their relations were also derived for the entire intervals of IWC and reflectivity values in their sets of in situ data. The IWP values for the relation that is specifically tuned for higher reflectivities ($Z_e > 0$ dBZ) are on average 55% higher than those obtained from the extended interval ($Z_e > -30$ dBZ) relation. It shows that the use of relations which were obtained with data dominated by small reflectivity and IWC values can result in significant biases when estimating ice contents of precipitating cloud systems.

5. Relating W Band Reflectivity and Optical Extinction Coefficient

[31] Optical extinction coefficient, α, and its vertical integral, optical thickness, τ, are very important properties that determine the radiative impact of clouds. Measurements of these parameters using optical (both passive and active) instruments aboard other A-train satellites flying in formation with CloudSat are, however, very limited (if not impossible) in thick precipitating cloud systems that result in rainfall. For such systems, CloudSat measurements can provide extinction estimates that would be useful retrieval information supplementing data from other satellites.

[32] It has been suggested previously [*Matrosov et al.*, 2003; *Hogan et al.*, 2006] that K_a band ($\sim$35 GHz) radars can be used for estimating vertical profiles of the extinction coefficient. Comparisons of the optical thicknesses obtained by integrating extinction profiles from a ground-based K_a band radar with the more direct and independent τ estimates from the Atmospheric Emitted Radiance Interferometer (AERI) for nonprecipitating ice clouds indicated a typical uncertainty of about a factor of 2 in radar based estimates [*Matrosov et al.*, 2003]. Such retrieval uncertainties are substantial because α and Z_e at K_a band are proportional to very different moments of PSD. At W band for stronger reflectivities that come primarily from particles with sizes that are outside the Rayleigh scattering regime, α and Z_e are proportional to more similar PSD moments. Thus CloudSat measurements can potentially provide useful estimates of extinction and optical thickness of ice parts of precipitating cloud systems.

[33] A scatterplot of extinction coefficient and W band radar reflectivity for ($r = 0.6$) is shown in Figure 8. Values of α were calculated from the data set described in section 3 using

$$\alpha(\mathrm{m}^{-1}) = 10^2 \sum_{i=1}^{n} 2N_i(D_i)A_i(D_i), \tag{6}$$

where A_i is the geometrical cross-sectional area (in cm^2) of an individual particle derived from 2-D images. The best fit power law approximation for the data in Figure 8 ($Z_e >$ 0 dBZ) is

$$\alpha(\mathrm{m}^{-1}) = 0.0014\, Z_e^{0.94}(\mathrm{mm}^6\,\mathrm{m}^{-3}), \tag{7}$$

Note that the exponents in (7) and in the Z_e-IWC relation (4) are quite similar. This is due to the fact that both α and IWC (given that bulk density is proportional to $D^{1.9}$) are proportional to similar moments of PSD.

[34] The relative bias and standard deviation of relation (7) are 8% and 52%, respectively. As for the Z_e-IWC relations discussed above, there is no significant temperature dependence in the Z_e-α relations for high values of reflectivity,

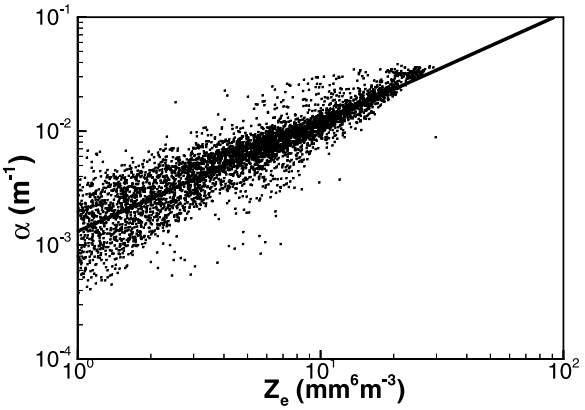

Figure 8. A scatterplot of visible extinction coefficient and W band reflectivity (r = 0.6).

which are the main interest of this study. The particle shape matters more. An assumption of more spherical particles with r = 0.8 rather than r = 0.6 results in an increase of the coefficient in (7) by about 30%, leaving the exponent (i.e., 0.94) practically unchanged.

[35] Estimating α from 2-D images using (6) does not account for the contribution from the smallest particles. While contributions from those particles to IWC estimates are small and typically can be neglected for particle populations with larger D_0 values, such contributions can be relatively more significant for extinction estimates [*Heymsfield et al.*, 2006b]. It may result in additional uncertainties/biases when using the relation (7). Nonetheless, estimates of the extinction coefficient and optical thickness from CloudSat reflectivity measurements could still be useful since they might be the only ones available in precipitating clouds. An example of optical thickness estimates are shown in Figure 7.

[36] *Comstock et al.* [2007, Figure 3b] show that the radar based approach to retrieve ice cloud optical thickness, where radar reflectivity based estimates of optical thickness τ were obtained using a relation from *Matrosov et al.* [2003], can compare satisfactorily with retrievals by optical methods for clouds with τ values that are greater than about 0.5. Their comparisons, however, were made for a nonprecipitating ice cloud. The appropriateness of using the relation that is specifically tailored for precipitating clouds observed by W band radar should be further tested with extinction retrieval data from other A-train sensors (for cases when measurements from these sensors are applicable).

6. Conclusions

[37] CloudSat appears to be a very valuable tool for observing precipitating systems from space. It presents a unique opportunity to provide vertically resolved information for the same atmospheric column on both rainfall and ice cloud phase above the melting layer. Since the use of optical remote sensors from other satellites that fly in formation with CloudSat (e.g., MODIS, lidar) is very limited for precipitating systems, the rainfall and ice cloud parameter retrievals need to rely on CPR reflectivity measurements. It is helped by the fact that attenuation of radar signals in ice phase is rather small compared to strong attenuation in liquid and melting phases [*Matrosov*, 2008].

[38] Ice cloud parts of precipitating systems are usually characterized by high values of observed radar reflectivity. For precipitating systems with rainfall rains, which are greater than a few mm h^{-1}, dominant contributions to the total ice content observed above the freezing level typically come from cloud volumes with Z_e values that are greater than 0 dBZ. Such high reflectivities at W band, typically result from larger ice particles, which are outside the Rayleigh scattering regime. The spherical model, which is often used to derive Z_e-IWC relations from cloud microphysical data sets, does not satisfactorily describe the backscattering properties of such particles.

[39] The need to derive Z_e-IWC relations specifically tuned for high reflectivity values was also dictated by the fact that existing relations were developed to cover a very large dynamic range of IWC values observed in a great variety of ice clouds ranging from thin cirrus to thick clouds with large particles. Since nonprecipitating cloud samples are typically more numerous, such relations might not necessarily provide best fits for precipitating clouds.

[40] A large microphysical data set collected during the CRYSTAL-FACE field campaign was used to derive a Z_e-IWC relation that is specifically tuned for higher reflectivities and is expected to be appropriate for applications with CloudSat measurements in ice cloud parts of precipitating systems that produce rainfall. A nonspherical ice particle model was used for this derivation. Aspect ratios for this model of about 0.6 appear to be appropriate for aggregated ice crystals as microphysical studies indicate. Such aspect ratios are also in agreement with dual-frequency radar measurements. The spherical model, which is often used to estimate aggregate particle reflectivities, is generally appropriate for smaller particle populations resulting in Z_e values that are less than about -10 dBZ. However, for higher Z_e values, which are typical for larger particle populations, this model can underestimate W band reflectivities by several dB.

[41] An important observation is that the data scatter in IWC-Z_e relations becomes progressively smaller as reflectivity increases, and individual points become confined to a relatively narrow area in ice water content–reflectivity scatterplots. This area is about the same for different data sets originating from various cloud types and geographical regions. This indicates that the derived relations are likely to be applicable to a wide variety of precipitating cloud systems. The reduced data scatter for higher reflectivities is, in part, a result of lesser influences of characteristic particle size on these relations due to strong non-Rayleigh scattering for the larger ice crystals, which are typical for ice parts of precipitating cloud systems. Typical values of median volume sizes of ice particle populations with Z_e > 0 dBZ are about 1–2 mm. Unlike for lower reflectivities, they vary relatively little and do not exhibit significant trends with Z_e, which also contributes to the low scatter in IWC-Z_e data points and to a larger exponent in power law approximations.

[42] While the variability of Z_e-IWC relations due to temperature for higher values of Z_e is rather small, the variability due to particle shape can be substantial, resulting in a bias in retrieved values of ice content on the order of

about 25%. A similar additional uncertainty (~30%) could result because of variability in the particle mass-size relations. Assuming independence in the IWC estimate variability due to data scatter (Figure 4) and due to the shape and mass-size relation assumptions, a total retrieval uncertainty could reach about 50%.

[43] Since optical sensors have serious limitations in retrieving visible extinction profiles in precipitating clouds, CloudSat can be useful in estimating the extinction coefficient α and optical thickness in such clouds. A Z_e-α relation was suggested for this purpose. This relation exhibits a greater data scatter compared to the Z_e-IWC relation. Estimates of extinction from cloud samples can also have more significant contributions from smaller particles (compared to the estimates of IWC and Z_e). This suggests that CloudSat extinction retrievals will likely have higher uncertainties compared to IWC retrievals. These uncertainties can easily by as high as a factor of 2 or so.

[44] Multiple scattering and attenuation of CloudSat signals in the ice phase might be a source of additional uncertainty in the retrievals. In ice devoid of cloud liquid water, however, attenuation is expected to be rather small except, probably, in the systems that produce very heavy rainfall. Such systems may also produce noticeable multiple scattering effects. A careful consideration of these effects for the CloudSat configuration deserves special study in future.

[45] **Acknowledgments.** This research was funded through the NASA CloudSat project (NNX07AQ82G). We wish to thank A. Bansemer (NCAR) for processing the microphysical data set.

References

Atlas, D., S. Y. Matrosov, A. J. Heymsfield, M. D. Chou, and D. B. Wolff (1995), Radar and radiation properties of ice clouds, *J. Appl. Meteorol.*, *34*, 2329–2345, doi:10.1175/1520-0450(1995)034<2329:RARPOI>2.0.CO;2.

Barber, P., and C. Yeh (1975), Scattering and attenuation by nonspherical atmospheric particles, *J. Atmos. Terr. Phys.*, *3*, 108–119.

Battaglia, A., M. O. Ajewole, and C. Simmer (2007), Evaluation of radar multiple scattering effects in CloudSat configuration, *Atmos. Chem. Phys.*, *7*, 1719–1730.

Bringi, V. N., and V. Chandrasekar (2001), *Polarimetric Doppler Weather Radar*, 636 pp., Cambridge Univ. Press, Cambridge, U. K.

Brown, P. R. A., and P. N. Francis (1995), Improved measurements of the ice water content in cirrus using a total-water probe, *J. Atmos. Oceanic Technol.*, *12*, 410–414, doi:10.1175/1520-0426(1995)012<0410:IMOTIW>2.0.CO;2.

Comstock, J. M., et al. (2007), An intercomparison of microphysical retrieval algorithms for upper tropospheric ice clouds, *Bull. Am. Meteorol. Soc.*, *88*, 191–204, doi:10.1175/BAMS-88-2-191.

Heymsfield, A. J., Z. Wang, and S. Matrosov (2005), Improved radar ice water content retrieval algorithms using coincident microphysical and radar measurements, *J. Appl. Meteorol.*, *44*, 1391–1412, doi:10.1175/JAM2282.1.

Heymsfield, A. J., A. Bansemer, S. L. Durden, R. L. Herman, and T. P. Bui (2006a), Ice microphysics observations in hurricane Humberto: Comparisons with non-hurricane generated ice cloud layers, *J. Atmos. Sci.*, *63*, 288–308, doi:10.1175/JAS3603.1.

Heymsfield, A. J., C. Schmitt, A. Bansemer, G. J. van Zadelhoff, M. J. McGill, C. Twohy, and D. Baumgardner (2006b), Effective radius of ice cloud particle populations derived from aircraft probes, *J. Atmos. Oceanic Technol.*, *23*, 361–380, doi:10.1175/JTECH1857.1.

Heymsfield, A. J., A. Bansemer, S. Matrosov, and L. Tian (2008), The 94 GHz radar dim band: Relevance to ice cloud properties and CloudSat, *Geophys. Res. Lett.*, *35*, L03802, doi:10.1029/2007GL031361.

Hogan, R. J., M. P. Mittermaier, and A. J. Illingworth (2006), The retrievals of ice water content from radar reflectivity factor and temperature and its use in evaluating a mesoscale model, *J. Appl. Meteorol. Climatol.*, *45*, 301–317, doi:10.1175/JAM2340.1.

Korolev, A., and G. Isaac (2003), Roundness and aspect ratio of particles in ice clouds, *J. Atmos. Sci.*, *60*, 1795–1808, doi:10.1175/1520-0469(2003)060<1795:RAAROP>2.0.CO;2.

L'Ecuyer, T. S., and G. L. Stephens (2002), An estimation-based precipitation retrieval algorithm for attenuating radars, *J. Appl. Meteorol.*, *41*, 272–285, doi:10.1175/1520-0450(2002)041<0272:AEBPRA>2.0.CO;2.

Li, L., G. M. Heymsfield, P. E. Racette, L. Tian, and E. Zenker (2004), A 94 GHz cloud radar system on a NASA high-altitude ER-2 aircraft, *J. Atmos. Oceanic Technol.*, *21*, 1378–1388, doi:10.1175/1520-0426(2004)021<1378:AGCRSO>2.0.CO;2.

Liu, C. L., and A. J. Illingworth (2000), Toward more accurate retrievals of ice water content from radar measurements of clouds, *J. Appl. Meteorol.*, *39*, 1130–1146, doi:10.1175/1520-0450(2000)039<1130:TMAROI>2.0.CO;2.

Matrosov, S. Y. (1997), Variability of microphysical parameters in high-altitude ice clouds: Results of the remote sensing method, *J. Appl. Meteorol.*, *36*, 633–648.

Matrosov, S. Y. (2007a), Potential for attenuation-based estimations of rainfall rate from CloudSat, *Geophys. Res. Lett.*, *34*, L05817, doi:10.1029/2006GL029161.

Matrosov, S. Y. (2007b), Modeling backscatter properties of snowfall at millimeter wavelengths, *J. Atmos. Sci.*, *64*, 1727–1736, doi:10.1175/JAS3904.1.

Matrosov, S. Y. (2008), Assessment of radar signal attenuation caused by the melting hydrometeor layer, *IEEE Trans. Geosci. Remote Sens.*, *46*(4), 1039–1047.

Matrosov, S. Y., M. D. Shupe, A. J. Heymsfield, and P. Zuidema (2003), Ice cloud optical thickness and extinction estimates from radar measurements, *J. Appl. Meteorol.*, *42*, 1584–1597, doi:10.1175/1520-0450(2003)042<1584:ICOTAE>2.0.CO;2.

Matrosov, S. Y., A. J. Heymsfield, and Z. Wang (2005), Dual-frequency radar ratio of nonspherical atmospheric hydrometeors, *Geophys. Res. Lett.*, *32*, L13816, doi:10.1029/2005GL023210.

Matrosov, S. Y., M. D. Shupe, and A. V. Djalalova (2008), Snowfall retrievals using mm-wavelength cloud radars, *J. Appl. Meteorol. Climatol.*, *47*, 769–777, doi:10.1175/2007JAMC1768.1.

Mitchell, D. L. (1996), Use of mass- and area-dimensional power laws for determining precipitation particle terminal velocities, *J. Atmos. Sci.*, *53*, 1710–1723.

Protat, A., J. Delanoe, D. Bouniol, A. J. Heymsfield, A. Bansemer, and P. Brown (2007), Evaluation of ice water content retrievals from cloud radar reflectivity and temperature using a large airborne in situ microphysical database, *J. Appl. Meteorol. Climatol.*, *46*, 557–572, doi:10.1175/JAM2488.1.

Sassen, K. (1987), Ice cloud content from radar reflectivity, *J. Clim. Appl. Meteorol.*, *26*, 1050–1053, doi:10.1175/1520-0450(1987)026<1050:ICCFRR>2.0.CO;2.

Sassen, K., S. Y. Matrosov, and J. Campbell (2007), CloudSat spaceborne 94 GHz radar bright band in the melting layer: An attenuation-driven upside-down lidar analog, *Geophys. Res. Lett.*, *34*, L16818, doi:10.1029/2007GL030291.

A. J. Heymsfield, National Center for Atmospheric Research, Boulder, CO 80307, USA.

S. Y. Matrosov, Earth System Research Laboratory, NOAA, R/PSD2, 325 Broadway, Boulder, CO 80305, USA. (sergey.matrosov@noaa.gov) z